

CODE BENCHMARKING OF LONG-TERM STORAGE OF HIGH INTENSITY BUNCHED BEAM

A. Engeda*, Goethe University Frankfurt, Frankfurt am Main, Germany

Y. Yuan, Institute of High Energy Physics, Beijing, China

G. Franchetti, GSI Helmholtz Centre for Heavy Ion Research, Darmstadt, Germany

Abstract

Most PIC solvers used in accelerator physics rely on 2D field models, which can limit accuracy for moderate to high intensity beams where space-charge effects dominate. A common approach to compute the self-consistent electric field in particle-based simulation codes is the use of a spectral Poisson solver based on FFT. In the "MICROMAP" library, a fully 3D FFT-based Poisson solver has been implemented. At the China Spallation Neutron Source (CSNS), an alternative technique based on tensor decomposition (TD-based) has been developed "TEST" (Tensor Element Symplectic Track). In this proceeding, we present a benchmark comparing the traditional FFT-based solver implemented in "MICROMAP" and the TD-based method for long-term tracking of high intensity bunched beams at low energy in the 3-dimensional space. We examine the differences in the beam rms dimension tracked over a long term.

INTRODUCTION

Space-charge effects are central in high intensity beam dynamics, significantly affecting the envelope evolution. In particle-in-cell (PIC) simulation, these effects are typically computed by depositing the particle charge onto a mesh, solving Poisson's equation calculating the smoothed electrostatic potential [1–3]. By differentiating the potential, one obtains the electric field. For realistic beam distributions, analytic solutions of Poisson's equation are difficult to determine, so numerical solvers are required. Among the most common approaches are FFT-based solvers and more recent TD-based methods [4, 5].

A benchmark of these two approaches is presented in the context of a PIC code with emphasis on numerical comparability. We compare the two solvers under identical beam and lattice parameters, focusing on long-term rms evolution.

Governing Equations

The electrostatic potential $\phi(\vec{x})$ generated by the beam charge density $\rho(\vec{x})$ satisfies Poisson's equation $\nabla^2 \phi(\vec{x}) = -\frac{\rho(\vec{x})}{\epsilon_0}$, where ϵ_0 is the vacuum permittivity. Once ϕ is computed, the electric field is obtained by $\vec{E}(\vec{x}) = -\vec{\nabla} \phi(\vec{x})$. In a PIC framework the charge density is represented on a mesh from macro-particles whose charge is deposited onto nearby grid points. Poisson's equation is then solved on that mesh and the resulting electric field is interpolated back into the position of the particles to update their momenta. This sequence is repeated over many time steps, making

the Poisson solver one of the dominant components in the computational load.

THEORETICAL FRAMEWORK

Spectral FFT Method

The classical spectral approach uses the fact that, under suitable boundary conditions, the discrete Laplacian is diagonalized on a Fourier basis. In the simplest free space or periodic setting, the potential can be solved by transforming the charge density into Fourier space, dividing by the wavenumber dependent Laplacian symbol, and transforming back to physical space. This makes FFT-based Poisson solvers particularly attractive because they avoid explicit assembly of large sparse matrices and can be implemented with very low algorithmic complexity per grid point.

For a uniform Cartesian grid, the method can be summarized as follows:

1. Deposit the charge density ρ in the mesh. Transform ρ into Fourier space using FFT.
2. Solve the algebraic relation for each mode, $\tilde{\phi}(\vec{k}) = -\frac{\rho(\vec{k})}{\epsilon_0 k^2}$.
3. Apply inverse FFT to recover the electric potential ϕ .
4. Compute the electric mean field $\vec{E} = -\vec{\nabla} \phi$, in physical space.

The strength of the FFT method is its speed. It is especially effective when the computational domain is rectangular and the boundary conditions are compatible with the transform basis. Its main limitations are reduced flexibility for complex geometries and the need for careful treatment of boundary conditions. In beam dynamics applications, FFT-based solvers are widely used because they provide a good balance of accuracy and computational cost for large scale simulations.

Tensor Decomposition Method

Tensor decomposition methods represent multidimensional arrays and operators in compressed low-rank format [4, 5]. Instead of storing the full 3D grid or operator explicitly, the method approximates them using factors whose size grows much more slowly with dimension. This is especially valuable in 3D Poisson problems, where the full tensor product structure can be expensive in memory and arithmetic cost.

Based on this method, we use tensor decomposition and n-mode product. The algorithm of TDM is following, first we obtain the charge density tensor $\hat{\rho} = K \times_1 U^{(1)} \times_2 U^{(2)} \times_3 U^{(3)}$ with PIC method and suppose the potential tensor $\hat{\phi} = S \times_1 U^{(1)} \times_2 U^{(2)} \times_3 U^{(3)}$, where the basis $U^{(1)}$, $U^{(2)}$ and

* engeda@iap.uni-frankfurt.de

$U^{(3)}$ with eigendecomposition based on different boundary condition.

Next define the right side tensor $A = -\hat{\rho}/\epsilon_0$ with the given boundary condition, Calculate the coefficient tensor K by $K = A \times_1 U^{(1)-1} \times_2 U^{(2)-1} \times_3 U^{(3)-1}$, and core tensor S can be expressed in the following,

$$S[i,j,k] = \frac{K[i,j,k]}{\lambda_x[i] + \lambda_y[j] + \lambda_z[k]} \quad (1)$$

Finally we have the potential map $\hat{\phi}$ via projecting S to $U^{(1)}$, $U^{(2)}$ and $U^{(3)}$. With the TDM method, we can deal with beam transport in different types of vacuum pipe, such as ellipse, circle, or other geometric boundaries.

SPECTRAL SOLVER VS. TENSOR DECOMPOSITION METHOD

Simulation Setup: Constant Focusing Ring and Bunched Beam

To compare the FFT-based and TD-based Poisson solver in a controlled setting, we consider a high intensity proton ring with constant focusing in the transverse plane at low energy. The ring is represented by a sequence of elements with identical phase advances. Space-charge kicks are applied at equally spaced interaction points around the ring. The initial bunched beam distribution is set to Waterbag in the transverse plane and in the longitudinal plane a Gaussian distribution truncated at 2σ . The bunch is represented by $N_p = 5 \times 10^4$ macro-particles. For the field solver, the computational domain is a 3D Cartesian box with an open boundary setting that represents the pipe in a storage ring.

Table 1: Initial Simulation Parameters

Parameter	Value	Unit
Bunch Population	5×10^9	-
RMS Emittance	10	mm · mrad
RMS Bunch Length	4	m
RMS dp/p	1×10^{-1}	-
Energy (Per Nucleon)	10	MeV
Lorentz Factor (γ_0)	1.01	-
Grid Resolution	$128 \times 128 \times 64$	-

Test Cases

Long-term tracking is performed for up to 5000 turns, corresponding to ten synchrotron periods. We investigate two scenarios for a high intensity beam in a constant focusing ring with a matched and a mismatched beam [6]. The initial conditions and lattice functions are equal where only the space-charge field solver differs.

For the matched case, the initial particle distribution is generated self-consistently including the effect of space-charge. This minimizes initial envelope oscillations and allows the comparison to focus on differences introduced by the numerical field solvers during long-term tracking.

For the mismatched case, the initial distribution is generated without space-charge matching. As a consequence, the beam is not in equilibrium with the self-consistent collective forces at the beginning of the simulation, leading to pronounced envelope oscillations and an initial redistribution of particles in phase space.

We track and compare the transverse rms beam sizes σ_x , σ_y , and the evolution of the longitudinal rms beam sizes σ_z as functions of turn number.

RESULTS

The evolution of the transverse and longitudinal rms beam sizes over 5000 turns is shown in Fig. 1 and 2.

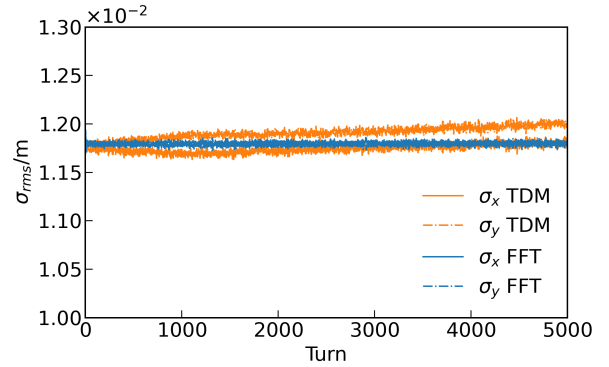


Figure 1: Evolution of the transverse RMS beam size over 5000 turns for the matched beam case (FFT-based vs. TD-based Poisson solvers).

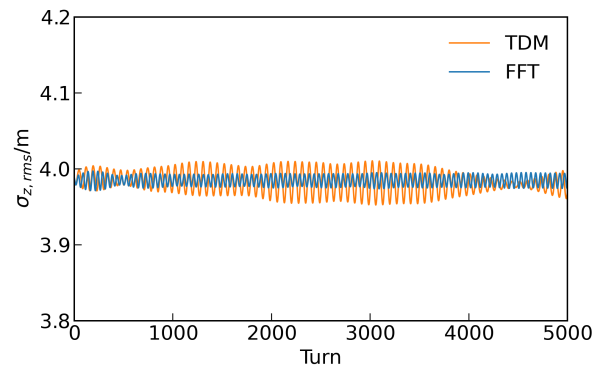


Figure 2: Evolution of the longitudinal RMS beam size over 5000 turns for the matched beam case (FFT-based vs. TD-based Poisson solvers).

Both the FFT-based solver and the TD-based method show a difference in transverse evolution. The benchmark reveals visible differences between the two numerical approaches. Deviations between the two approaches become visible after several hundred turns.

The longitudinal evolution shows differences in the synchrotron oscillation phase between the two solvers during long-term tracking. Figures 3 and 4 show a zoom in to the first 100 turns for the matched and mismatched beam cases, respectively. During the initial turns, the mismatched

beam exhibits stronger envelope oscillations caused by the inconsistency between the initial distribution and the self-consistent space-charge forces while the matched beam remains initially closer to equilibrium and therefore shows reduced oscillation amplitudes.

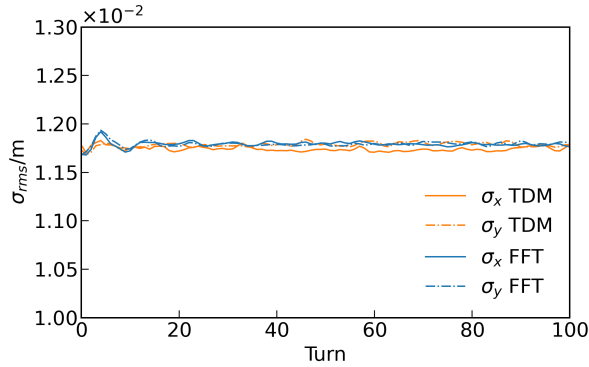


Figure 3: Transverse RMS beam size during the first 100 turns for the matched beam case. The initial distribution remains close to the matched condition, resulting in reduced envelope oscillations.

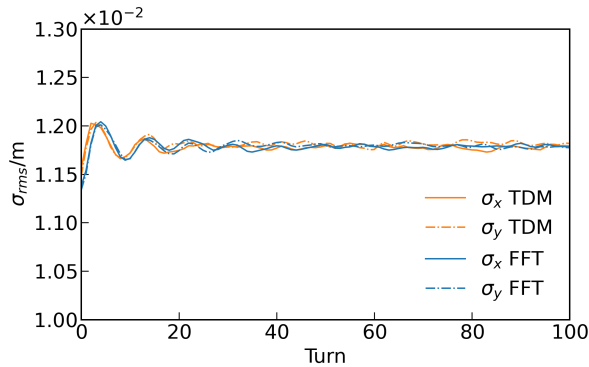


Figure 4: Transverse RMS beam size during the first 100 turns for the mismatched beam case. Stronger initial envelope oscillations are observed due to the mismatch between the generated distribution and the matched condition. After several turns, the beam relaxes toward a quasi-stationary state similar to the matched case.

After 50 turns, the influence of the initial mismatch becomes significantly reduced. This indicates that the beam undergoes a redistribution in phase space driven by space-charge effects.

CONCLUSION

This benchmark compares the FFT-based Poisson solver implemented in "MICROMAP" with the tensor-decomposition-based solver in "TEST" for long-term tracking of high-intensity bunched beams at low energy. Both methods are able to simulate the evolution of matched and mismatched beams in a 3D self-consistent PIC setting. The comparison shows that the two solvers agree qualitatively in the early stage of the tracking, especially in the relaxation behavior of the mismatched beam, but noticeable differences appear in the rms beam size evolution after several hundred turns.

These deviations suggest that further investigation is needed to quantify numerical differences between the solvers.

ACKNOWLEDGMENTS

This work is jointly supported by the National Natural Science Foundation of China (Grant No. 12475155), the Guangdong Basic and Applied Basic Research Foundation (Project No. 2024A1515012658) and the International Partnership Program of Chinese Academy of Sciences (Project No. 013GJHZ2023026FN).

REFERENCES

- [1] R. W. Hockney and J. W. Eastwood, "Computer simulation using particles", 1966. <https://api.semanticscholar.org/CorpusID:60571788>
- [2] D. Fortunato and A. Townsend, "Fast poisson solvers for spectral methods", *IMA J. Numer. Anal.*, vol. 40, no. 3, pp. 1994–2018, Jul. 2020. [doi:10.1093/imanum/drz034](https://doi.org/10.1093/imanum/drz034)
- [3] L. Greengard and V. Rokhlin, "A fast algorithm for particle simulations", *J. Comput. Phys.*, vol. 73, no. 2, pp. 325–348, 1987. [doi:10.1016/0021-9991\(87\)90140-9](https://doi.org/10.1016/0021-9991(87)90140-9)
- [4] J. Y. Du, X. N. Du, X. G. Liu, and Y. S. Yuan, "3d space charge solver based on tensor decomposition for high-intensity beams", *Prog. Theor. Exp. Phys.*, vol. 2025, no. 4, p. 043G01, Apr. 2025. [doi:10.1093/ptep/ptaf047](https://doi.org/10.1093/ptep/ptaf047)
- [5] Q. Thai Tran, D. P. Truong, Kim Ø Rasmussen, and B. Alexandrov, "A tensor train-based isogeometric solver for large-scale 3d poisson problems", *Comput. Methods Appl. Mech. Eng.*, vol. 453, p. 118802, 2026. [doi:10.1016/j.cma.2026.118802](https://doi.org/10.1016/j.cma.2026.118802)
- [6] G. Franchetti, "Space Charge in Circular Machines", *CERN Yellow Rep. School Proc.*, vol. 3, p. 353, 2017. [doi:10.23730/CYRSP-2017-003.353](https://doi.org/10.23730/CYRSP-2017-003.353)